CONF

CONF-810804--13

MASTER

POST-TEST ANALYSIS OF DRYOUT TEST 7B' of the W-1 SODIUM LOOP SAFETY FACILITY EXPERIMENT WITH THE SABRE-2P CODE

S. D. Rose and J. F. Dearing

Oak Ridge National Laboratory
Oak Ridge, Tennessee 37830

(Submitted for presentation at the 20th National ASME-AIChE Heat Transfer Conference, August 2-5, 1981, Milwaukee, Wisconsin)

Research sponsored by the Division of Reactor Research and Technology U. S. Department of Energy under contract W-7405-eng-26 with the Union Carbide Corporation.

POST-TEST ANALYSIS OF DRYOUT TEST 7B' OF THE W-1 SODIUM LOOP SAFETY FACILITY EXPERIMENT WITH THE SABRE-2P CODE

S. D. Rose and J. F. Dearing

Oak Ridge National Laboratory
Oak Ridge, Tennessee 37830

An understanding of conditions that may cause sodium boiling and boiling propagation that may lead to dryout and fuel failure is crucial in liquid-metal fast-breeder reactor safety. In this study, the SABRE-2P subchannel analysis code has been used to analyze the ultimate transient of the in-core W-1 Sodium Loop Safety Facility experiment. This code has a 3-D simple non-dynamic boiling model which is able to predict the flow instability which caused dryout. In other analyses dryout has been predicted for out-of-core test bundles and so this study provides additional confirmation of the model.

EXPERIMENT DESCRIPTION

The SLSF W-1 experiment (Ref. 1 and 2) was designed to evaluate the heat release characteristics of fast reactor fuel pins under loss-of-piping integrity (LOPI) accident conditions and determine stable boiling initiation and recovery limits (the boiling window) in a prototypic fuel pin bundle. The SLSF in-core loop is a doubly-contained closed sodium test vehicle and is located in the Engineering Test Reactor (ETR) at the Idaho National Engineering Laboratory (INEL). A 19-pin bundle with Clinch River Breeder Reactor (CRBR) type axial blankets is located in the 7.9 m long test train which is instrumented by thermocouples, pressure transducers and flowmeters. In addition, the center seven fuel pins have annular fuel pellets over the length of the active section and in-fuel thermocouples. The outer 12 pins have solid pellets, with fuel enrichments selected to produce a flat power profile.

The fuel pins are 5.84 mm in diameter spaced by 1.42 mm diameter wire-wrap spacers on the inner seven pins and 0.71 mm diameter wire-wrap spacers on the outer 12 pins. The half-size edge gaps help flatten the radial temperature profile across the bundle to give a better simulation of the central region of a full size subassembly. The stainless steel hexcan is 1.02 mm thick and surrounded by a layer of alumina insulator and an outer containment tube. The bypass coolant flows by means of small tubes located outside the

outer tube (Fig. 1). Each fuel pin has a thermocouple in its respective wire-wrap and the thermocouples are positioned at various axial locations. The attrition rate was unfortunately high and for this final test 7B' of the W-1 series, only 6 of the 19 wire-wrap thermocouples were operating.

Dryout test 7B' was a controlled flow reduction transient at 679 kW total power. This was the only test in this series to reach dryout. Approximately two seconds of coolant boiling were observed, starting near the top of the fueled section of the bundle and propagating down to the core axial midplane and growing radially across the whole bundle cross-section. Peak wire-wrap thermocouple temperatures exceeded 1100°C and peak fuel temperatures exceeded 2500°C with no post-transient test section flow blockage being detected, indicating just incipient fuel pin failure and no apparent fuel melting. A summary of the principal occurrences for this test are given in Table 1. In the study with SABRE-2P analysis is up to the onset of dryout at 2.7 seconds when the inlet flow decays to zero.

SABRE-2P BOILING MODEL

SABRE-2 (Ref. 3) is a Liquid Metal Fast Breeder Reactor (LMFBR) thermal-hydraulic subchannel analysis code that has a transient single-phase capability. A simple non-dynamic boiling model has been added to this code; the modified version referred to as SABRE-2P. This code has already provided an accurate three-dimensional representation of transient boiling behavior to dryout for forced flow and natural convection runs at lower power in 19-pin and 61-pin out-of-core test bundles operated on the Thermal-Hydraulic Out-of-Reactor Safety (THORS) facility at Oak Ridge National Laboratory (ORNL) (Ref. 4).

The code solves the fully three-dimensional conservative equations in subchannel geometry. SABRE-2 is based on the semi-implicit calculation method MAC (Ref. 5) in which the velocity and heat equations are solved explicitly in time and only the pressure equation (deduced from the mass balance equation) is solved implicitly. This procedure results in a time step limitation by the Courant condition on the flow which may be replaced by a fully implicit solution method in later versions of the code. The time dependent thermo-hydraulic equations for incompressible flow are solved, and the code is suitable for calculating single phase flows, and as modified at ORNL in SABRE-2P, can deal with homogeneous boiling.

TABLE 1

W-1 SLSF Experiment Dryout Test 7B′ Summary of Events

Time (sec)	Events
0	Start of Controlled Flow Reduction Transient
0.5	Test Section Inlet Flow Reaches Reduced Level
1.5	Approximate Time of Boiling Inception Near Top of Fueled Section
2.1	Complete Cross-section of Bundle Boiling; Static Instability Causes Flow to Start to Decay
2.7	Inlet Flow Decays to Zero Value
2.8	Inlet Flow Reversal and Start of Test Section Flow Oscillations
3.1	Boiling Progression to Fuel Bundle Axial Midplane
3.5	Reactor Scram; Dryout Observation Across Top of Fuel Region
3.8	Inlet Flow Recovery
4.1	Peak Wire-Wrap Thermocouple Temperature Exceed 1100°C Peak Fuel Thermocouple Temperature Exceed 2500°C
4.6	Inlet Flow Back to Full Flow Conditions

The essential features of the SABRE-2P boiling model are:

1. The two-phase quality is calculated on the basis of subchannel enthalpy and used to calculate a subchannel two-phase friction factor multiplier (homogeneous viscosity corrected) for inclusion in the axial momentum equation.

2. The subchannel quality is also used to calculate a void fraction (slip = 1) which is used to modify the gravitational body force term in the axial momentum equation.

3. Thermal conductivity, density, and viscosity are evaluated as liquid properties at the saturation temperature, however, the enthalpy field solved by the energy equation is that of the two-phase mixture (or, equivalently, a superheated liquid).

The density change on boiling is not included in the continuity equation. Reasons for not doing this include the following:

a. Inclusion of this term results in flow oscillations and these are extremely hard to model numerically, even in one dimension.

b. Adequate correlations for interphase heat and momentum transfer during these flow oscillations do not exist.

c. Experimental results from THORS out-of-core boiling tests at ORNL (Ref. 4) suggest that the dynamic behavior plays only a small role in determining dryout behavior.

These oscillations about the mean flow are instead viewed as enhanced two-phase turbulence which affects the effective thermal diffusivity of the boiling region.

SABRE-2P MODEL OF W-1 BUNDLE

A one-twelfth section model of the test bundle was used in the analysis and is shown in Fig. 2. Nodes 1 through 4 represent the subchannel arrangement used in the SABRE-2P thermal-hydraulic analysis and nodes 5 through 12 represent the one-dimensional thermal conduction subchannel of the bundle housing that was coupled to the subchannel model. This subroutine is called

at each axial level at each time step. The input argument is the temperature of the edge subchannel (node 4) and the output is the heat flux from the hex-can (node 5) to the edge subchannel.

Twenty-four axial nodes each of length 0.1143 m are used: three upstream of the fuel section, eight for the 0.914 m fueled section and thirteen upstream for the upper blanket and fission gas plenum region. A wire-wrap forced diversion crossflow model is not used in this version of SABRE, but the value for the turbulence mixing multiplier used in the code corresponds to a value found suitable from analyses with THORS Bundle 6A (Ref. 6), which is a 19-pin out-of-core bundle with very similar geometry to the W-1 bundle. Subchannel areas and wetted perimeters are corrected on an average basis for the presence of the wire-wraps.

In the version of SABRE used here, there is only a simple fuel pin model. The heat source into the coolant is represented by a simple two region model for the fuel pins and the coolant, assuming a linear solution to the heat-transfer between them. Transverse thermal conduction through the fuel pins was represented by using a value of 1.5 for the thermal conduction shape factor which was calculated using a finite difference scheme for internal subchannels (Ref. 7).

In modeling the controlled flow reduction SABRE-2P utilizes a transient pressure drop boundary condition for solving the fully three-dimensional conservation equations in subchannel geometry. The test-section pressure drop was reduced from the steady-state value at $t = 0$ seconds to the low flow value at $t = 0.45$ seconds and then held constant (0.45 seconds $< t <$ 3 seconds). The experimental conditions for Test 7B′ are given in Table 2. The inlet resistance due to the flow restrictions to the test bundle is represented as a $K\rho V^2$ term on the first axial node. Pressure drop investigations indicate that a value of $K = 11.2$ is suitable (Ref. 8) and a mean sodium saturation temperature of 966°C was used. The computer running time for this problem is about 450 seconds on an IBM 3033 using a storage of about 250 K bytes; the Courant condition on the flow being a large influence on this time.

ANALYSIS

Figure 3 shows the experimental test section inlet flow and the inlet flow predicted by SABRE-2P up to 2.7 seconds into the transient when the flow

TABLE 2

W-1 Test 7B′ Experimental Conditions

Initial flow	2.3 ℓ/s (t = 0s)
Low flow	0.85 ℓ/s (t = 0.5s)
Power	35.74 kW/pin
Inlet temperature	388°C

decays to zero as indicated in Table 1. The wire-wrap thermocouple instrumentation indicates that the inception of boiling at the end of the fueled section, centrally in the bundle is detected at about 1.5 seconds and that the complete cross-section of the bundle reaches boiling at about 2.1 seconds. The static (Ledinegg) flow excursion then occurs causing the flow to decay to a zero value at 2.7 seconds. This flow instability is predicted by SABRE-2P and leads to dryout which was detected about 0.8 seconds later. SABRE-2P predicts the time of boiling initiation at about 0.6 seconds, whereas the limited thermocouple instrumentation indicates a value of about 1.5 seconds. Post-test data analysis of the W-1 experiment by COBRA-3M also consistently predicts boiling initiation earlier than measured in the boiling window tests (Ref. 9). The difference in SABRE-2P may be attributed to the simple fuel pin model used and is discussed further; the main occurrence, the flow decay instability to dryout is predicted at the correct time, and the sensitivity of this to different experimental parameters has been determined.

Figure 4 shows the variation in the SABRE-2P inlet flow prediction to (1) the effective heat transfer coefficient of the fuel pins, (2) the effective thermal conductivity of the alumina insulation and (3) the initial flow value in the controlled flow reduction. The simple fuel pin heat transfer model consists of two regions - the fuel or structure region and the coolant region, and two parameters - an effective heat transfer coefficient and a heat capacity parameter for the fuel pins. The heat capacity parameter is the heat capacity of the structure associated with each subchannel, in units J m^{-1} K^{-1}. The heat transfer model assumes a mean heat source per unit axial length in the fuel (P_L W m^{-1}), which is transferred to the coolant proportionally to the temperature difference between the two regions (ΔT K):

$$P_L = H\Delta T$$

where H is the effective heat transfer coefficient (W m^{-1} K^{-1}). Thermocouples from only three of the fuel pins produced sensible temperature records in the Test 7B′ transient and these gave a value of H in the range 10 to 14 W m^{-1} K^{-1}. To determine the sensitivity of the calculation, H has been varied by a reasonable amount, H = 11 $\pm$ 6 W m^{-1} K^{-1} (H = 11 W m^{-1} K^{-1} corresponds to a $\Delta T \sim$ 1600°C). This variation in the effective heat transfer coefficient of the fuel pins produces a variation in the time of the Ledinegg instability of 2.1 $\pm$ 0.4 seconds.

The effective thermal conductivity of the alumina insulation surrounding the hexcan (EF) was varied in the calculation. EF is defined as the ratio of the thermal conductivity of the insulation to the thermal conductivity of sodium. EF = 0.17 corresponds to the thermal conductivity of alumina at 600°C; this temperature being found suitable from available thermocouple data for the insulation. The variation shown is for EF = 0.19 (500°C) and EF = 0.13 (800°C) and only corresponds to a variation of $\pm$ 0.1 seconds to the time of the Ledinegg instability.

The SABRE-2P calculation was also repeated for a variation in the low flow value of 0.85 $\pm$ 0.03 ℓ/s in order to show the sensitivity of the calculation to a reasonable range in the flow measurement. The flow characteristic is basically the same with a variation of $\pm$ 0.25 seconds to the time of the flow instability. The variations to these different experimental parameters did not change the predicted time to boiling inception significantly; for example, H = 11 $\pm$ 6 W m^{-1} K^{-1} gave a boiling time of 0.62 $\pm$ 0.04 seconds.

The SABRE-2P model shows the three-dimensional flow diversion around the developing boiling region and the rapid reduction of the inlet flow when the boiling region encompasses the entire cross-section. This is illustrated in Fig. 5, which shows the approximate development of the boiling region at 2 seconds. Arrows on this figure indicate velocity vectors at a few positions in the bundle. Also shown are the locations of three wire-wrap thermocouples in the bundle and the thermocouple in the hexcan used in the radial temperature comparisons that follow.

Figure 6 shows the experimental and predicted radial temperature profiles near the end of the fueled section of the bundle during the transient. The thermocouples are located at slightly different axial locations (see Fig. 5), and the SABRE-2P values are corresponding to these respective locations. Three profiles are shown, the steady-state temperature profile (t = 0 seconds), the profile at t = 1 second, and at 2.1 seconds when the boiling region encompasses the complete bundle cross-section. Notice that the SABRE-2P prediction shows a steeper radial profile at t = 1 second, during the development of the boiling region. The existence of the increasing temperature profile shown experimentally indicates radial heat loss through the hexcan. The influence of a more flat steady-state temperature profile which is essentially a more one-dimensional problem was considered in the SABRE-2P calculation by increasing the turbulent mixing and changing the inlet velocity profile.

The turbulent mixing parameter in SABRE-2P was increased by a factor of one hundred, and as expected the time to boiling initiation was increased (to about 1.8 seconds), but the flow curve was not significantly altered with the flow instability occurring again at about 1.2 seconds. The effect of a non uniform inlet velocity profile was considered because upstream to the inlet to the bundle is located the inlet flowmeter which has a diameter of only about half that of the bundle hexcan. The sudden expansion at the inlet to the bundle may cause the velocity to be higher towards the center of the bundle and hence make the radial temperature field more one-dimensional. This geometric effect was implemented in SABRE-2P by using extra axial nodes upstream to the heated section of the bundle and modeling a blockage at the appropriate location. The calculation had little effect on the inlet flow curve, but the boiling inception time was increased from 0.6 seconds to 0.9 seconds. These results suggest that two-dimensional considerations are important and dominant, since in both runs discussed the significant occurrence is the Ledinegg instability which is correctly predicted.

The code predicts the effect of boiling on the axial flow. The two-phase friction multiplier tends to decrease the flow locally in the boiling region, and the gravitational body term tends to increase the flow. The boiling model is able to calculate the transient flow redistribution around and through the boiling region as it grows axially and radially, and the resulting change in total inlet flow produced by a constant pressure drop boundary condition. The explanation for this appears to be that the increased axial two-phase resistance of the homogeneous multiplier produces the correct axial distribution of transverse mass flux into and out of the boiling region. The transverse convection term is the dominant term in the energy balance in the boiling region until it completely encompasses the bundle cross-section. Note that the model predicts neither the correct density or transverse velocity, but does predict correctly their product, the transverse mass flux, which convects the enthalpy.

Using data from a central wire-wrap thermocouple the time of boiling inception was estimated to be about 1.5 seconds. The transient data was adjusted for this thermocouple to correct for the effects of reversed leads in the W-1 instrument connector (see Appendix D, Ref. 2). This correction is

substantiated by comparison with another thermocouple at the same elevation but a different radial position in the bundle. In addition, there may be a small correction to be applied to allow for the time constant of the thermocouple. As mentioned, the boiling time has been predicted by SABRE-2P at 0.6 seconds. It was found by changing the value for the fuel pin heat capacity parameter that the heat transferred to the coolant from the fuel initially, at the start of the transient is too great. The simple two-region model for the structure and the coolant appears to be insufficient for fast transients in nuclear fuel pins, but has been shown to be suitable for transients in THORS bundles. In fuel pin simualtors, the temperature gradient from the pin center to its edge is far less steep and so is easier to model. A more detailed representation of the thermal characteristics of the fuel pins has been implemented in a later version, SABRE-2A (Ref. 10). The simple fuel pin model in SABRE-2P is adequate, however, in showing the flow instability to dryout for Test 7B' and this has been found to be not too sensitive to the initial time of boiling inception.

SUMMARY AND CONCLUSIONS

Subchannel code SABRE-2P with a simple non-dynamic boiling model was used to analyze the dryout Test 7B' of the SLSF W-1 experiment. The code correctly predicts the static (Ledinegg) flow excursion which starts at about 2.1 seconds into the transient once the entire bundle cross section has reached boiling. This flow excursion leads to film dryout after 2.7 seconds when the flow reaches zero. These results indicate that the boiling behavior is determined by two-dimensional considerations. The code predicts boiling initiation earlier than measured, probably due to its simple fuel pin model and shows a steeper radial temperature profile across the bundle during the development of the boiling region. The sensitivity of the SABRE-2P prediction to different experimental parameters - variation in the low flow, effective heat transfer coefficient of the fuel pins, and effective thermal conductivity of the insulation shows a maximum variation 2.1 ± 0.4 seconds in the time to the Ledinegg instability. Dryout has also been correctly predicted by SABRE-2P for lower power runs in THORS out-of-core test bundles. Thus, the same occurrence in the W-1 SLSF in-core experiment reported in this analysis provides additional confirmation of the model.

REFERENCES

1. J. M. Henderson et al, *W-1 SLSF Experiment LOPI Transient and Sodium Boiling Tests - Description and Interim Results*, HEDL-TC-1497 (June 1980).

2. J. M. Henderson, *W-1 SLSF Experiment Data Record*, HEDL-TC-1738 (June 1980).

3. J. D. MacDougall, *SABRE-2: A Computer Program for the Calculation of Transient Three-Dimensional Flows in Rod Clusters*, UKAEA, AEEW-R1104, (July 1978).

4. R. J. Ribando et al, *Sodium Boiling in a Full-Length 19-Pin Simulated Fuel Assembly (THORS Bundle 6A)*, ORNL/TM-6553 (January 1979).

5. J. E. Welch et al, *The MAC Method. A Computing Technique for Solving Viscous Incompressible, Transient Fluid Flow Problems Involving Free Surfaces*, LA-3425 (1965).

6. M. H. Fontana and J. L. Wantland, *ORNL LMFBR Safety and Core Systems Programs Progress Report for January-March 1977*, ORNL/TM-5940 (August 1977).

7. M. H. Fontana and J. L. Wantland, *ORNL Breeder Reactor Safety Quarterly Technical Progress Report for July-September 1979*, ORNL/TM-7229 (May 1980).

8. J. M. Henderson, HEDL, Private Communication, (October 9, 1980).

9. D. D. Knight, GEC, Sunnyvale, Private Communication, (November 25, 1980).

10. J. D. MacDougall, *SABRE-2A: A Version of the SABRE Computer Program for Calculating Transient Three-Dimensional Flows in Rod Clusters Including the VUDS Differencing Scheme and Calculation of Pin and Structure Temperatures*, UKAEA, FRGN 702, (February 1979).

ACKNOWLEDGEMENTS

Research sponsored by the Division of Reactor Research and Technology U.S. Department of Energy under contract W-7405-eng-26 with the Union Carbide Corporation.

Figure Captions

Fig. 1 Cross-Section of the W-1 SLSF Experiment in the Lower Test Section Region (from Ref. 1, HEDL-TC-1497).

Fig. 2 One-Twelfth Section SABRE-2P Model of the W-1 SLSF Experiment.

Fig. 3 Test Section Inlet Flow W-1 SLSF Experiment Test 7B′ - Experimental Data and SABRE-2P Results.

Fig. 4 Test Section Inlet Flow W-1 SLSF Experiment, Test 7B′ - SABRE-2P Results Showing Sensitivity of: (1) Effective Heat Transfer Coefficient of Fuel Pins,(2) Effective Thermal Conductivity of Insulation, (3) Low Flow Value.

Fig. 5 Development of the Boiling Region at 2 seconds in W-1 SLSF Experiment, Test 7B′.

Fig. 6 W-1 SLSF Experiment, Test 7B′ Radial Temperature Profile Across the Bundle Near the End of the Fuel Section - Experimental Data and SABRE-2P Results.

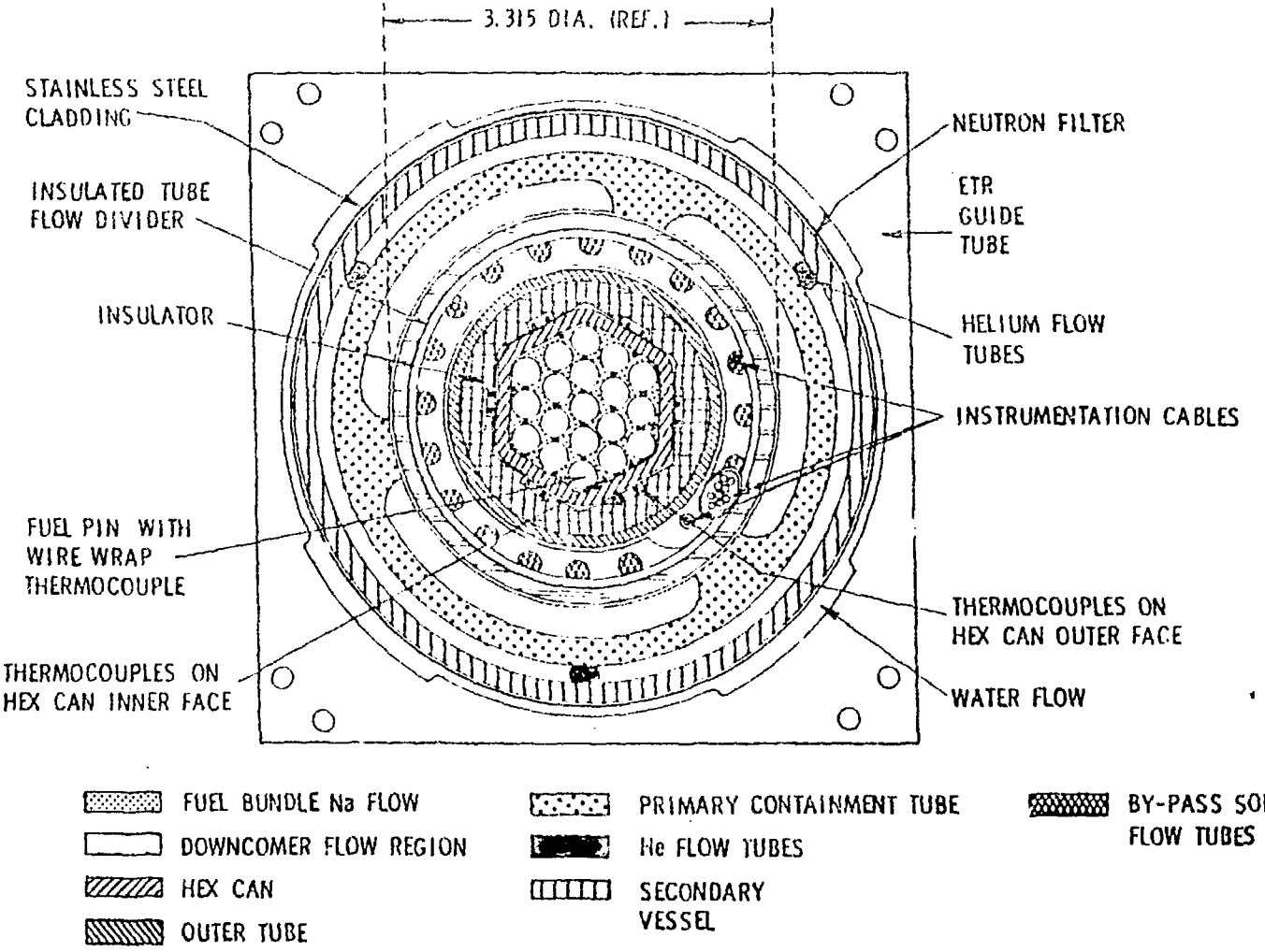

HEDL 7701-62.1

Fig. 1

Fig. 2

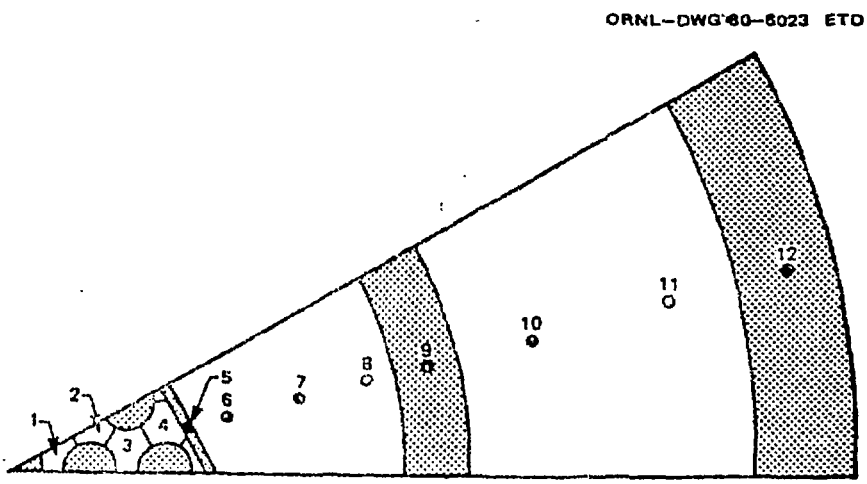

Fig. 1.1. One-twelfth-section thermal-hydraulic model of THORS Bundle 6Av.

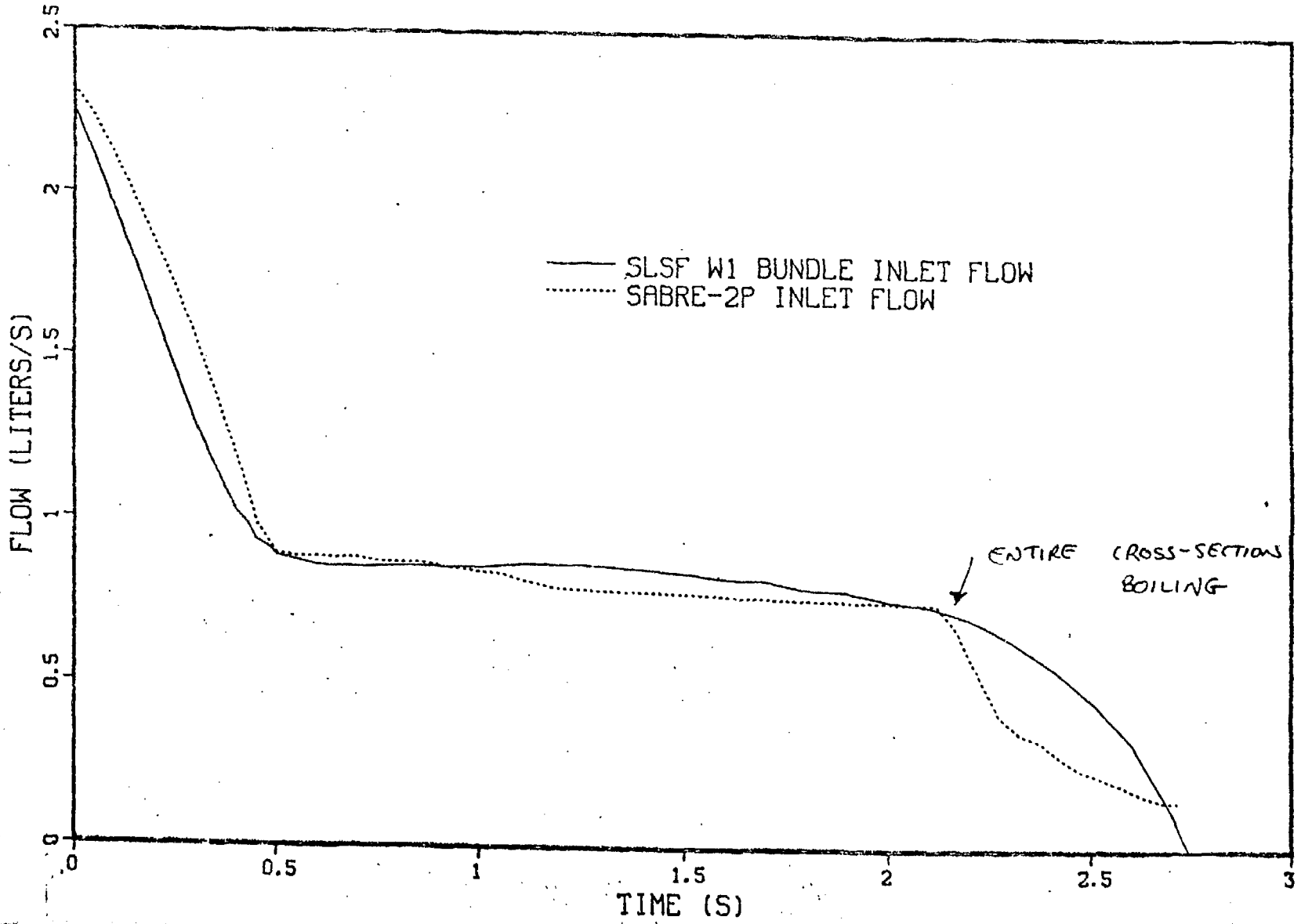
SLSF W1 BUNDLE INLET FLOW
SABRE-2P INLET FLOW
ENTIRE CROSS-SECTION BOILING
FLOW (LITERS/S)
TIME (S)
0
0.5
1
1.5
2
2.5
3

Fig. 3

Fig. 4

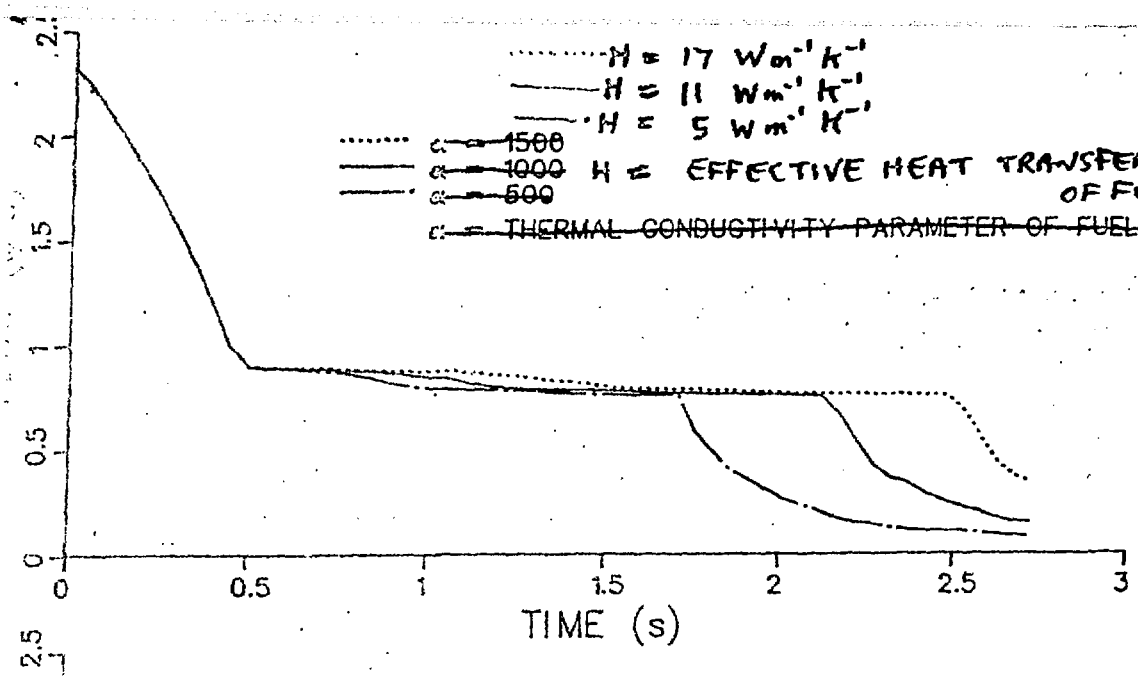
H = 17 Wm⁻¹K⁻¹
H = 11 Wm⁻¹K⁻¹
H = 5 Wm⁻¹K⁻¹
H = EFFECTIVE HEAT TRANSFER COEFFICIENT OF FUEL PINS
TIME (s)

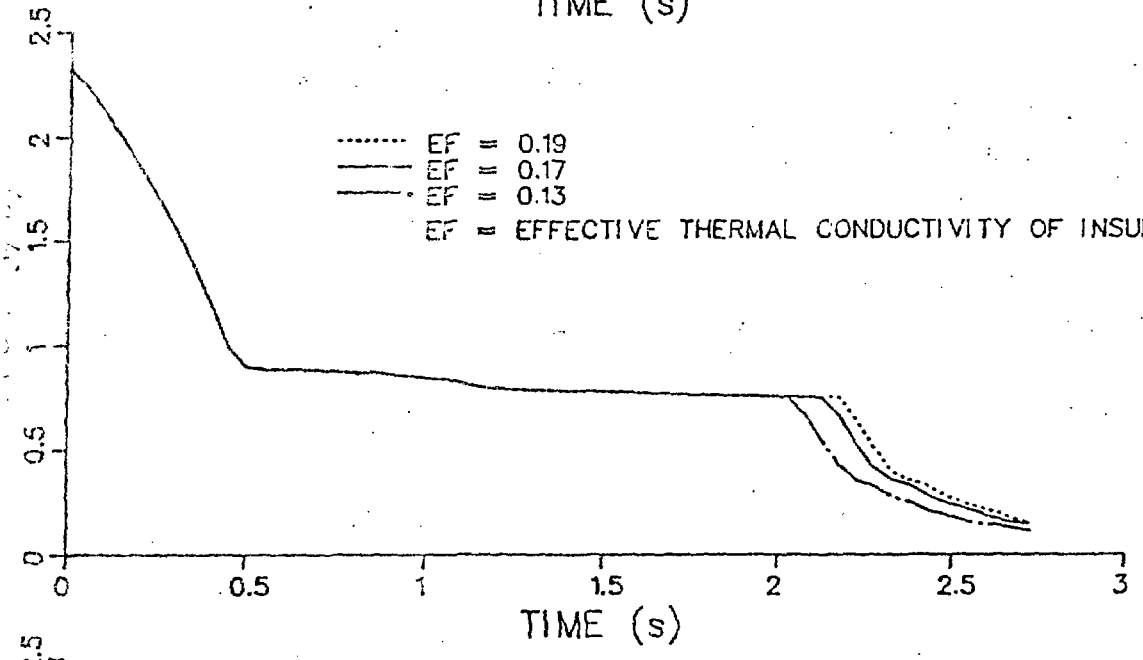
EF = 0.19
EF = 0.17
EF = 0.13
EF = EFFECTIVE THERMAL CONDUCTIVITY OF INSULATION
TIME (s)

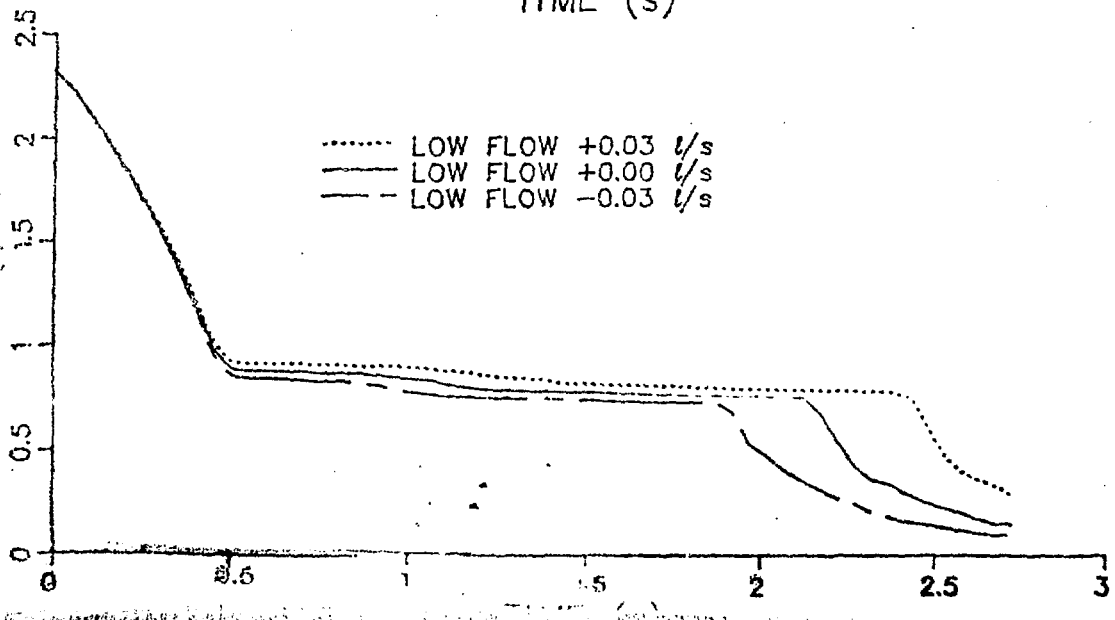
LOW FLOW +0.03 l/s
LOW FLOW +0.00 l/s
LOW FLOW −0.03 l/s

Fig 5.

Fig. 5.

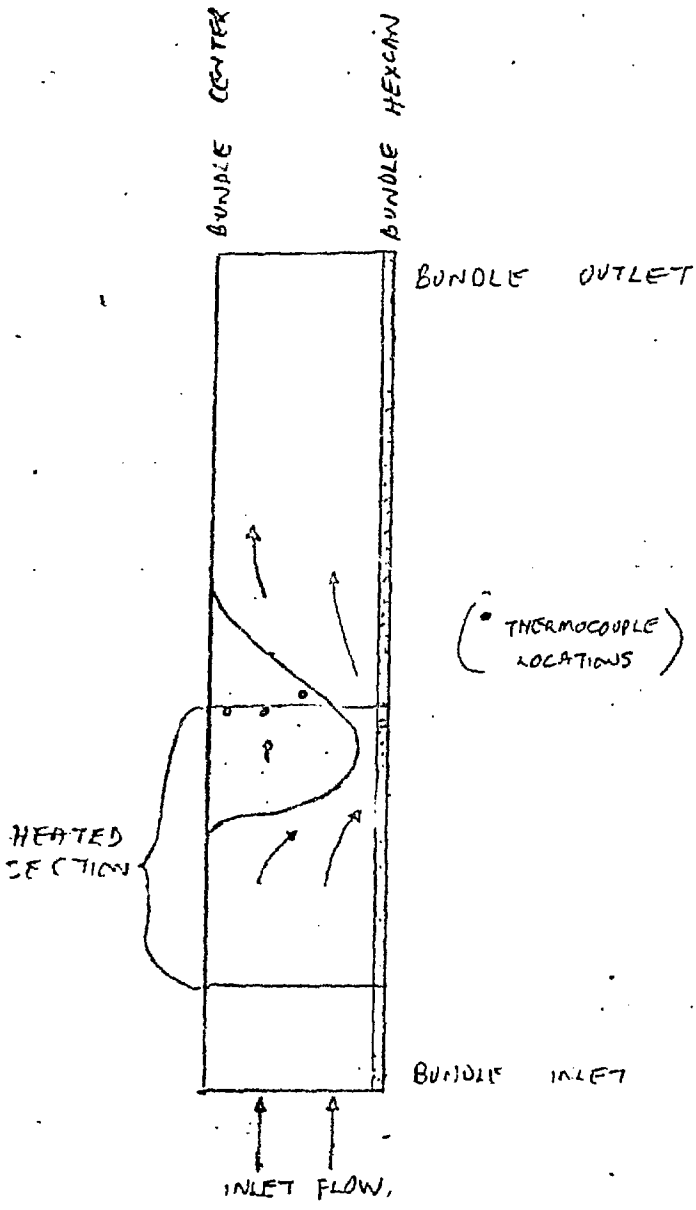
BUNDLE CENTER
BUNDLE HEXCAN
BUNDLE OUTLET
THERMOCOUPLE LOCATIONS
HEATED SECTION
BUNDLE INLET
INLET FLOW,

Fig 6.

SLSF W1 TEST 7B'
SABRE-2P
t = 0 s
t = 1 s
t = 2.1 s
Bundle CENTER
Bundle HEXCAN
Bundle CENTER
Bundle HEXCAN
500
600
700
800
900
TEMPERATURE (DEG. C)